Acta Physica Polonica B Proceedings Supplement **18**, 5-A7 (2025)

ELECTROWEAK MEASUREMENTS AT THE CMS EXPERIMENT: RECENT RESULTS*

Luca Della Penna

on behalf of the CMS Collaboration

INFN and University of Perugia. Dipartimento di Fisica
Via Alessandro Pascoli, snc, 06123, Perugia, Italy

Received 31 March 2025, accepted 5 May 2025, published online 26 June 2025

Electroweak measurements are a key part of the CMS Collaboration's physics program, enabling precise measurements of known observables. These measurements are crucial for placing stringent limits on Standard Model parameters providing insights into New Physics. Presented here are some of the latest results from the CMS Collaboration, including the first results using Run 3 data collected at $\sqrt{s} = 13.6$ TeV in 2024.

DOI:10.5506/APhysPolBSupp.18.5-A7

Introduction

Electroweak (EW) measurements are essential to the physics program of the CMS experiment [1], as they involve gauge bosons and photons. These measurements cover a wide range of cross-section magnitudes and rare processes, such as Vector Boson Fusion (VBF) and Vector Boson Scattering (VBS). EW measurements not only impose stringent constraints on the Standard Model (SM) parameters, but also provide a means to explore potential effects beyond the Standard Model (BSM). In this article, a selection of the results from 2024 in the EW sector is presented. In Section 1, the CMS detector is briefly presented. Section 2 is dedicated to searches focused on the extraction of Standard Model (SM) parameters, followed by the presentation of cross-section extraction results in Section 3. Finally, studies that investigate potential BSM effects are discussed.

* Presented at the 31st Cracow Epiphany Conference on the *Recent LHC Results*, Kraków, Poland, 13–17 January, 2025.

1. CMS apparatus

The CMS experiment [1] is one of the two general-purpose experiments at the LHC. Its central component is a superconducting solenoid with an internal diameter of 6 meters, which generates a magnetic field of 3.8 T. The solenoid volume houses a silicon pixel and strip tracker, a lead tungstate crystal electromagnetic calorimeter (ECAL), and a brass and scintillator hadron calorimeter (HCAL), each consisting of a barrel and two endcap sections. Forward calorimeters extend the pseudorapidity coverage provided by the barrel and endcap detectors. Muons are detected using gas-ionization chambers, which are embedded in the steel flux-return yoke outside the solenoid.

2. SM parameters extraction

2.1. EW mixing angle

The distribution of the final-state leptons in Drell–Yan processes serves as a proxy for extracting the electroweak mixing angle. Due to the axial and vector current interference, the mixing angle θ_{EW} can be measured by looking at the forward–backward asymmetry, *i.e.*, the difference in the cross section of dilepton production from the Z boson in the two hemispheres of the detector. To date, the most precise measurements of the mixing angle come from LEP and SLD analyses [2]. In the CMS published result [3], using Run 2 data at $\sqrt{s} = 13$ TeV, the Drell–Yan process with a muon or an electron in the final state is used by requiring two light opposite-charged leptons from the Z bosons decay. In contrast with measurements coming from e^+e^- colliders, the uncertainty in a hadron collider is dominated by the parton distribution functions (PDFs): due to the different couplings of the Z boson to up-type and down-type quarks, the PDF predictions for the relative contribution of each quark affect the forward–backward asymmetry. Furthermore, the relative angle to the incoming quark of the negative-charged lepton is defined from the boosted dilepton system, resulting in a dependence from the parton fraction. Results are summarized in figure 1, where $A_{\mathrm{FB}}^{w}(|y|, m)$ denotes the weighted asymmetry (equal to the normalized $\sigma_{\mathrm{F}} - \sigma_{\mathrm{B}}$, if computed in the full phase space), as already used in a previous analysis by the CMS Collaboration [4]. The other quantity, $A_{\mathrm{FB}}^{4}(|y|, m)$, represents the contribution coming from the differential cross section as in equation (1), all the other terms can be neglected

$$\frac{\mathrm{d}\sigma}{\mathrm{d}\cos\theta \mathrm{d}\Phi} \sim 1 + \cos^2\theta + \sum_{i=0}^{7} A_i f_i\left(\theta, \phi\right) \,. \tag{1}$$

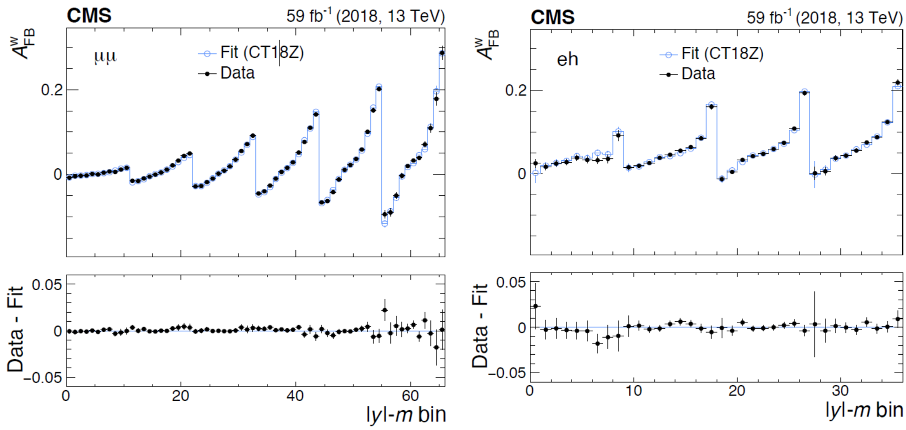

Fig. 1. Values of $A^w_{\rm FB}$ for $\mu^+\mu^-$ and e^+e^- for each of the mass and rapidity bin using the CT18Z set [5]. In the right plot, *eh* stands for an electron reconstructed using also HCAL information.

To date, the result obtained in [3], $\sin^2\theta_W = 0.23157 \pm 0.00031$, represents the most precise measurement at a hadron collider. The major source of uncertainty comes from the PDF, variations of $A_4(|y|, m)$ for different PDF sets can be seen in figure 2. This result is comparable to those from SLD and LEP, and helps to resolve the discrepancy between these two measurements, which differ by 3.2σ.

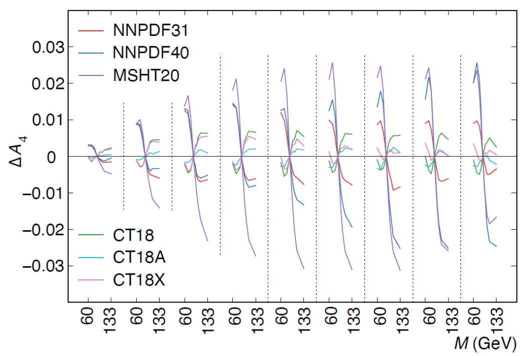

Fig. 2. Variation of A_4 with respect to the nominal configuration (CT18Z) in the different M bin of the dilepton system when different PDF sets are chosen. Outside the Z peak, the asymmetry receives a contribution from the interference of the two diagrams for $Z/\gamma \to l^+l^-$ dilepton production.

2.2. W-boson branching fraction ratio

The universality of weak interactions in the quark sector is a consequence of the unitarity of the Cabibbo–Kobayashi–Maskawa (CKM) matrix. A test of the CKM matrix can be performed by examining the quantity R_c^W, defined as the ratio of the branching fraction $\mathrm{BR}(W \to cq)$ to the sum of $\mathrm{BR}(W \to cq) + \mathrm{BR}(W \to uq)$. Unitarity predicts this ratio to be 0.5. The most precise measurement of this value was made using the full Run 2 data-taking period, achieving twice the precision of previous results [6]. The analyzed final state is the semileptonic decay of a $t\bar{t}$ pair, where each top quark decays into a W boson and a bottom quark, with the presence of a charm quark originating from the W boson decay. Jets originating from the hadronization of charm are selected using a muon-based technique: about $\sim 9\%$ of charmed-hadron decays producing a muon. This method enabled the calibration of the strategy directly on data, using b-jets from the semileptonic decays of b-hadrons, which allowed for a precise measurement of the branching ratio. The muon is required to have an opposite sign compared to the lepton from the decay of the other W boson from the $t\bar{t}$ pair, along with the isolation of the muon within the jet cone. Tagged and non-tagged charm events distinguish the contributions coming from $W \to cq$ or $W \to uq$ decay. The measured value of R_c^W is found to be $R_c^W = 0.489 \pm 0.020$, with the value of the squared elements in the second row of the CKM matrix equal to $\sum_i |V_{ci}| = 0.970 \pm 0.041$.

3. Cross section extraction

Since the beginning of LHC operations, CMS has measured the cross section of multi-boson production at all the energies reached by the collider. With the beginning of the Run 3 data taking-period in 2022, the centre-of-mass energy of 13.6 TeV was reached. During the last year, the cross section for the inclusive $W^{\pm}W^{\mp}$ and $W^{\pm}Z$ productions has been measured. Figure 3 summarizes the results of two papers [7, 8]. For WZ productions, the final state is tagged by requiring three isolated light leptons ($p_{\mathrm{T}}^{\mathrm{lep}} > 15$ or 25 GeV) with at least two opposite-sign leptons produced by the decay of the Z bosons. A constraint on $|m_{l_1,l_2} - m_Z| < 15$ GeV is required to isolate the signal from the background contributions, such as ZZ or $t\bar{t}Z$ productions. The final result is $\sigma(pp \to WZ) = 55.2 \pm 1.2\,(\text{stat.}) \pm (\text{sys.}) \pm 0.8\,(\text{lumi.}) \pm 0.1\,(\text{theory})$, in agreement with the SM prediction. For W^+W^- inclusive cross section, two isolated, high-p_{T}, oppositely charged leptons, including those coming from τ decay are selected. The result, $\sigma(pp \to WW) = 125.7 \pm 2.3\,(\text{stat.}) \pm 4.8\,(\text{sys.}) \pm 1.8\,(\text{lumi.})$ pb, is found to be in agreement with the theoretical SM prediction.

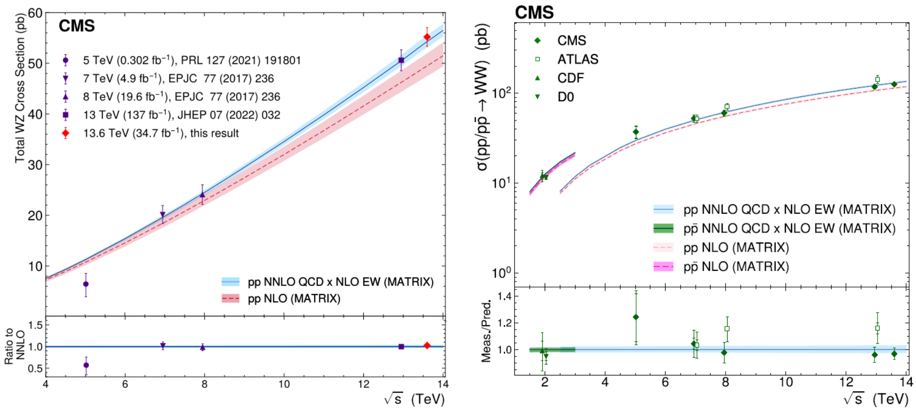

Fig. 3. Total cross section for WZ (left) and WW (right) as measured by the CMS Collaboration at the different energies reached by LHC, compared with NNLO QCD X NLO EW and NLO predictions from MATRIX [9].

4. Searches for beyond Standard Model effects

Searches for New Physics are often conducted within the framework of Effective Field Theory (EFT) [10]. In this approach, the SM Lagrangian is considered as the low-energy theory of a more general theory, defined at a scale $\Lambda_{\mathrm{BSM}} \gg \Lambda_{\mathrm{SM}}$. The resulting Lagrangian, assuming an expansion of New Physics that includes dimension-6 and dimension-8 operators, can lead to couplings of higher dimensions. Recent results from the CMS Collaboration have placed constraints on these operators, encoded in the Wilson coefficients, by investigating VBS and elastic $\gamma\gamma \to \tau\tau$ processes.

4.1. Vector boson scattering

VBS is the SM process with the lowest cross section measured by the CMS Collaboration ever. Since the first observation of the fully leptonic golden channel $W^{\pm}W^{\pm}$ by ATLAS [11] and CMS [12], increasing attention has been focused on this class of processes, where the existence of BSM effects could lead to anomalous triple gauge couplings (TGC) or quartic gauge couplings (QGC).

The first analysis to include a τ lepton in the final state, along with a BSM interpretation of the results, was published in 2024 [13]. The study used data from Run 2, with a total of 128 fb^{-1}, and focused on the decay chain $W^{\pm}W^{\pm} \to l^{\pm}\nu_l\tau_h^{\pm}\nu_\tau$, where τ_h stands for a τ lepton decaying hadronically. Despite the clean topology of a VBS event (two high-p_{T} and well-separated jets in the backward–forward direction), there is an irreducible

QCD background, which necessitates the inclusion of additional variables. The selection criteria for the final state requires at least two "VBS" jets and exactly one light lepton and one same-sign τ lepton. In figure 4, the output of a Deep Neural Network (DNN) in the signal region is shown. The full list of the variables used can be found in the original paper [13] among these, the Zeppenfeld variable [14] is used as a proxy for jet separation of VBS-like processes, while transverse mass variables are used for the energy of the scattering W pair and angular distribution of their decay products. These last variables are useful particularly to isolate possible EFT contributions, as shown in figure 5.

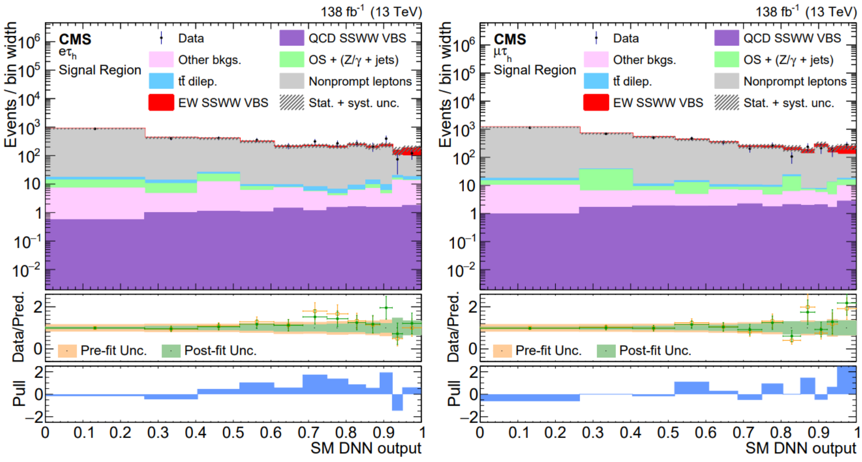

Fig. 4. Stacked DNN output distribution for $e\tau_h$ and $\mu\tau_h$ final states: the signal strength is obtained by fixing the contribution of the QCD VBS WW production to the SM prediction (purple), isolating the pure SM EW contribution (red). The middle panel shows the ratio of data to background, while the bottom panel shows the pulls distribution.

This represents the first study of a VBS process with a τ lepton in the final state, resulting in a signal strength of $1.44^{+0.63}_{-0.56}$ relative to the SM with a significance of 2.6σ. Beyond the Standard Model measurements, possible contributions from higher-dimensional EFT operators are explored, and constraints are placed separately on the Wilson coefficients by considering only one active operator at a time for dim-6 and dim-8 operators. Additionally, constraints are derived for two dim-6 operators and a combination of one dim-6 and one dim-8 operator using a log-likelihood scan of one coefficient against the other. These are the first limits obtained in VBS processes with two active dim-6 operator at the same time and the first ever with a combination of one dim-6 plus one dim-8 operator.

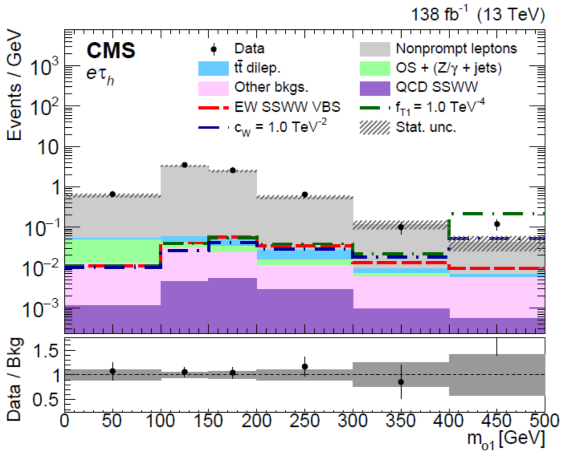

Fig. 5. Distribution of $m_{\circ 1}$ transverse mass for $e\tau_h$ final state. Here, $m_{\circ 1}$ is defined as the transverse mass of the $l\tau_h$ pair as if it is produced from a null invariant mass system. The solid green line and the blue line show the shape of dim-6 and dim-8 operators, respectively, while the red line shows the SM VBS signal.

4.2. Observation of $\gamma\gamma \to \tau\tau$

In [15], a pure QED process is explored, involving the production of two τ leptons via photon–photon fusion. In the case where the colliding protons remain intact (*i.e.*, no dissociation), the signature of the process will be two back-to-back leptons with no hadronic activity, except for the tagged hadronically decayed τ-leptons. To match this topology, the main variables used are acoplanarity, which accounts for the "back-to-back" requirement, and the low number of tracks at the dilepton vertex, regarding the "protons remain intact" condition. The final states, to avoid background from $\gamma\gamma \to ee$ and $\gamma\gamma \to \mu\mu$, is defined to be $e\mu$, $\tau_h\tau_h$, $e\tau_h$, $\mu\tau_h$. In the extraction of the signal, contributions from single and double dissociation are taken into account, isolating only the elastic contribution to the process. To fulfill this requirement, the $\mu\mu$ final state is used in order to derive a scaling factor directly from data, giving that in the single and double dissociation, the events satisfy the track and acoplanarity requirement in a lower number of cases. The observed fiducial cross section, extracted only in the $N_{\text{tracks}} = 0$ condition is found to be $\sigma_{\text{fid}} = 12.4^{+3.8}_{-3.1}$ fb^{-1}, as depicted in figure 6 (left), where a clean excess of events can be seen in the first bin. This result is found to be in agreement with the GAMMA-UPC generator [16]. Other than the observation of the $\gamma\gamma \to \tau\tau$ process, possible EFT contributions are searched.

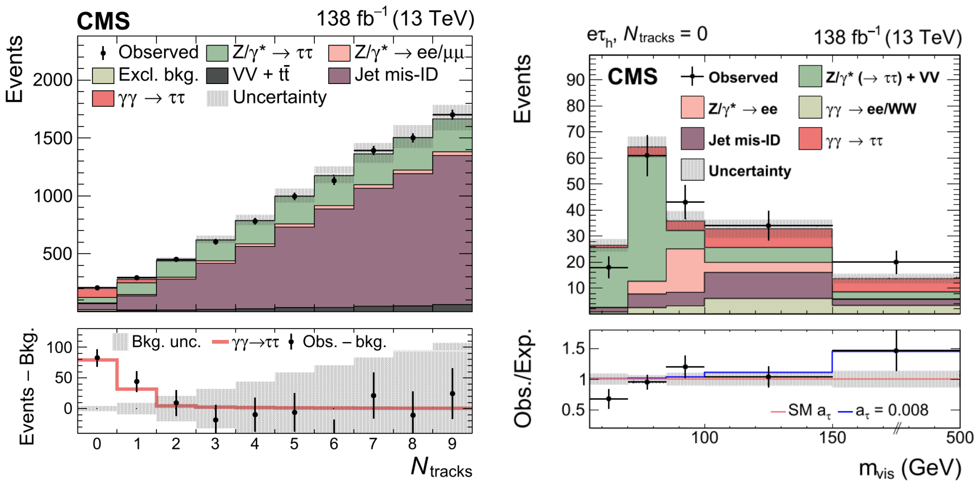

Fig. 6. (Left) Background-subtracted signal for all the possible final states taken into account, with the requirement of a $m_{\mathrm{vis}} > 100$ GeV of the reconstructed $\tau\tau$ lepton to reduce the background from DY dilepton production. (Right) Effect of the BSM contribution to a_τ (blue line): the number of expected events will increase as a function of the mass of the reconstructed $\tau\tau$, here shown for the $e\tau_h$ final state. The value of $a_\tau = 0.008$ is for explanation purpose only.

The most general form of photon–lepton vertex is

$$\Gamma^\alpha = \gamma^\alpha F_1\left(q^2\right) + \frac{\sigma^{\alpha\beta}q_\beta}{2m}\left[iF_2\left(q^2\right) + F_3(q^2)\gamma^5\right] . \tag{2}$$

If EFT contributions are taken into account, the anomalous magnetic moment a_τ, as well as the anomalous electric dipole moment d_τ, modify with a dependence on the real and imaginary parts of the Wilson coefficient, respectively. This will result in a dependence of the anomalous magnetic moment from the mass value of the $\tau\tau$ system, as depicted in figure 6 (right). The extracted values of the anomalous magnetic moment is $a_\tau = 0.0009^{+0.0032}_{-0.0031}$, while the constraint on the electric dipole moment $|d_\tau| < 2.9 \times 10^{-17}$ $e$cm, in agreement with the SM predictions. At present, this result is the most stringent limit on the magnetic moment of the τ lepton. Constraints on the Wilson coefficients are reported in figure 7.

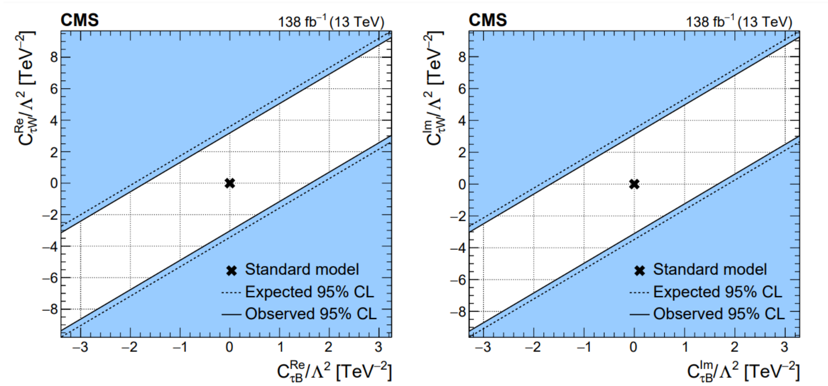

Fig. 7. Constraints on the real and imaginary parts of the Wilson coefficients. BSM effects will result in a modification of $\delta a_\tau \propto \mathrm{Re}[C_{\tau\gamma}]$ and $\delta d_\tau \propto \mathrm{Im}[C_{\tau\gamma}]$. The figure shows the expected and observed 95% C.L. constraints, while the blue bands are the excluded regions.

Summary

A selection of the latest results from the CMS Collaboration in the electroweak sector has been presented. These include precise measurements for the extraction of Standard Model parameters, cross-section extractions, and searches for rare processes and New Physics beyond the Standard Model. No excess has been observed in the search for BSM effects within the context of an Effective Field Theory. Additionally, the first EW analysis using Run 3 data is also presented.

REFERENCES

[1] CMS Collaboration (S. Chatrchyan *et al.*), *J. Instrum.* **3**, S08004 (2008).

[2] The ALEPH Collaboration, The DELPHI Collaboration, The L3 Collaboration, The OPAL Collaboration, The SLD Collaboration, The LEP Electroweak Working Group, The SLD Electroweak and Heavy Flavour Groups, *Phys. Rep.* **427**, 257 (2006).

[3] CMS Collaboration, *Phys. Lett. B* **866**, 139526 (2025), `arXiv:2408.07622 [hep-ex]`.

[4] CMS Collaboration, *Eur. Phys. J. C* **78**, 1 (2018).

[5] T.-J. Hou *et al.*, *Phys. Rev. D* **103**, 014013 (2021).

[6] CMS Collaboration, `arXiv:2412.16296 [hep-ex]`.

[7] CMS Collaboration (A. Hayrapetyan *et al.*), *J. High Energy Phys.* **2025**, 115 (2025), `arXiv:2412.02477 [hep-ex]`.

[8] CMS Collaboration, *Phys. Lett. B* **861**, 139231 (2025).
[9] M. Grazzini, S. Kallweit, M. Wiesemann, *Eur. Phys. J. C* **78**, 537 (2018).
[10] W. Buchmüller, D. Wyler, *Nucl. Phys. B* **268**, 621 (1986).
[11] ATLAS Collaboration (G. Aad *et al.*), *Phys. Rev. Lett.* **113**, 141803 (2014).
[12] CMS Collaboration (A.M. Sirunyan *et al.*), *Phys. Rev. Lett.* **120**, 081801 (2018).
[13] CMS Collaboration, `arXiv:2410.04210 [hep-ex]`.
[14] D. Rainwater, R. Szalapski, D. Zeppenfeld, *Phys. Rev. D* **54**, 6680 (1996).
[15] CMS Collaboration, *Rep. Prog. Phys.* **87**, 10 (2024).
[16] H.-S. Shao, D. d'Enterria, *J. High Energy Phys.* **2022**, 248 (2022).